Alternative Analytical Solution for Position and Orientation in Electromagnetic Motion Tracking Systems

MURILO TEIXEIRA SILVA
Department of Electrical and Computer Engineering
Memorial University of Newfoundland
St. John's, NL, A1B 3X5
CANADA
murilots@mun.ca

EDUARDO TELMO FONSECA SANTOS
Departamento de Automação e Sistemas
Instituto Federal de Educação, Ciência e
Tecnologia da Bahia (IFBA).
R. Emídio dos Santos,S/N,Barbalho.
Salvador/BA.41310-015.
BRAZIL
eduardot@ifba.edu.br

JOSÉ MÁRIO ARAÚJO
Departamento de Automação e Sistemas
Instituto Federal de Educação, Ciência e
Tecnologia da Bahia (IFBA).
R. Emídio dos Santos, S/N, Barbalho
Salvador/BA.41310-015.
BRAZIL
jomario@ifba.edu.br

LURIMAR SMERA BATISTA
Instituto Federal de Educação, Ciência e
Tecnologia da Bahia (IFBA).
Departamento de Matemática
R. Emídio dos Santos,S/N, Barbalho
Salvador/BA.41310-015.
BRAZIL
lurimar@ifba.edu.br

Abstract: An alternative analytical solution to six degrees-of-freedom position and attitude estimation problem is proposed. The proposed method relies on the use of Singular Value Decomposition to the transformation matrix between the currents in the transmitter and in the receiver. The proposed method is validated using synthetic data, in which a random motion is applied to the transmitter within an environment with different levels of noise. Once the efficacy of the method is confirmed, the proposed algorithm is benchmarked against a well established closed-form solution. The presented method was able to accurately obtain the position and orientation, with performance comparable to the benchmark.

Key–Words: Electromagnetic Sensor, Motion Tracking, Analytical Solution, Parameter Estimation

1 Introduction

Six degrees-of-freedom (6-DOF) position and attitude estimation is a problem that frequently arises in computer vision and robotics, in which it is desired to determine the position and orientation of a given object, in relation to a reference frame. Electromagnetic (EM) trackers have been widely studied and recently used in applications that require a high level of accuracy, such as image-guided surgery and other medical applications [13, 3, 10, 15, 11], as well as in virtual reality and motion capture [6, 2]. To obtain an accurate position, calibration techniques were developed to reduce environment interference and other sources of error [7] or alternative approaches for coil settings [4]. However, the pose estimation methods have not changed in the same pace.

The pioneering paper on 6-DOF EM motion tracking [12] describes an algorithm to find the position and orientation of an electromagnetic motion tracker recursively using linear transformations and rotation matrices. Later, matrix closed-form solutions and iterative approximations using quaternion-based methods were developed [8]. Closed form solutions are desirable over numeric approximations since they are non-iterative, which increases the processing speed.

The present work proposes an alternative analytical solution to the position and orientation estimation problem in 6-DOF electromagnetic Tracking systems using Singular Value Decomposition (SVD). The method is non-iterative, which provides a fast and accurate solution.

2 Preliminaries

2.1 Electromagnetic Motion Tracker

The system herein discussed is the same proposed in [12] and [8]. It consists in a two sets of three-axis orthogonal coils, one acting as a source and other as a sensor. The objective of this system is to identify the relative position and orientation between source and sensor, as shown in Fig. 1. Sensor position is represented in spherical coordinates (α_1,β_1,ρ), relative to source reference, while sensor orientation is determined by Euler angles (ϕ_1, θ_1, ψ_1). Using the notation presented in [12], the subscript indicates the coordinate frame which the variable is related; variables with subscript 1 are referenced to source coordinate frame, while the subscript 5 indicates that the variable is related to the sensor coordinate frame. The distance ρ does not have a subscript since this variable does not depend on the coordinate frame [12].

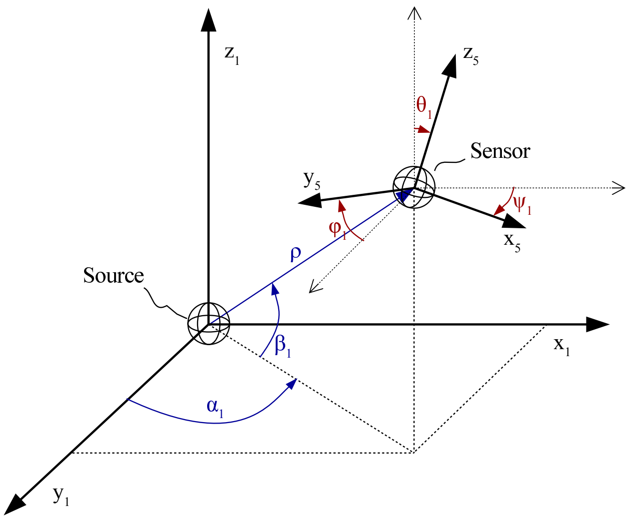

Figure 1: Position (in blue) and Orientation (in red) parameters in a 6-DOF Electromagnetic Motion Tracking system

By exciting a N-turns coil with a variable current of amplitude I, a magnetic dipole field is created, with magnetic moment $\boldsymbol{\mu}$ described by (1), where $\boldsymbol{\Omega}$ is the surface vector of the coil, with the same direction of the normal vector $\mathbf{n}$, defined by the right hand rule. For a circular coil with radius r, $\boldsymbol{\Omega} = \pi r^2 \mathbf{n}$.

$$\boldsymbol{\mu} = NI\boldsymbol{\Omega} \tag{1}$$

For a sufficiently small loop ($\rho >> r$), the magnetic field generated at an arbitrary point $P(\rho, \alpha, \beta)$ in the near field region ($k\rho << 1$, where k is the wavenumber) can be described by the radial and tangential components alone. The equations (2) and (3) presents the magnitude of the radial and tangential components of the magnetic field at a point P [1].

$$H_r(\rho, \beta) = \frac{\mu}{2\pi\rho^3} \cos\beta \tag{2}$$

$$H_t(\rho, \beta) = \frac{\mu}{4\pi\rho^3} \sin\beta \tag{3}$$

Faraday's Law states that placing another coil at point P, the variable magnetic field will induce a induced current over it. Since the strength of the field is a function of the relative position between the excited (source) and induced (sensor) coils, it is possible to deduce P from the source and sensor currents. By using three concentric coils in both source and sensor, with their magnetic moments mutually perpendicular, it is possible to obtain the relative position and orientation between source and sensor. Usually, source and sensor have the same parameters, such as number of coil turns and surface area.

The excitation of the source happens in three sequential excitation states. Each state is represented by a vector, where each component stands for the current value for the orthogonal coils at the given state. The excitation sequences must have linearly independent states, in order to be readily identifiable. The simplest example of excitation sequence is the excitation of only one coil at each state.

The magnetic field generated by each source excitation state generates a corresponding set of induced currents in the sensor. In vector notation, $\mathbf{f_1^{(n)}}$ stands for the source excitation currents vector at a given n state, while $\mathbf{f_5^{(n)}}$ is the sensor induced currents vector at the same n excitation state. They can be amalgamated into two matrices, $\mathbf{F_1}$ and $\mathbf{F_5}$, as shown in (4) and (5).

$$\mathbf{F_1} = \left[\mathbf{f_1^{(1)}}\mathbf{f_1^{(2)}}\mathbf{f_1^{(3)}}\right] = \begin{bmatrix} f_{1x}^{(1)} & f_{1x}^{(2)} & f_{1x}^{(3)} \\ f_{1y}^{(1)} & f_{1y}^{(2)} & f_{1y}^{(3)} \\ f_{1z}^{(1)} & f_{1z}^{(2)} & f_{1z}^{(3)} \end{bmatrix} \tag{4}$$

$$\mathbf{F_5} = \left[\mathbf{f_5^{(1)}}\mathbf{f_5^{(2)}}\mathbf{f_5^{(3)}}\right] = \begin{bmatrix} f_{5x}^{(1)} & f_{5x}^{(2)} & f_{5x}^{(3)} \\ f_{5y}^{(1)} & f_{5y}^{(2)} & f_{5y}^{(3)} \\ f_{5z}^{(1)} & f_{5z}^{(2)} & f_{5z}^{(3)} \end{bmatrix} \tag{5}$$

Both source and sensor are connected to a computing unit, that runs an algorithm to estimate position and orientation from the given current vectors. The algorithm is executed after each sequence of three excitation states [12]. After three excitation states, it is possible to build the source excitation and sensor induced matrices, that contain sufficient information to determine the relative position and orientation between source and sensor.

The electromagnetic coupling between source and sensor can be described as a linear transformation between source to sensor coordinate frames [12]. By using spherical coordinates, rotation is one of the main elements for the determination of the relative position and orientation between source and sensor. Any rotation can be expressed as a rotation matrix.

A rotation of an angle γ around a u-axis can be written in matrix form as $\mathbf{R}^u_\gamma$. Any rotation matrix can be seen as a combination of canonical rotation matrices, which have rotation axis in the same direction of the unit vectors of the Cartesian coordinate frame. The canonical rotation matrices for an arbitrary rotation angle γ are shown in Table 1.

Table 1: Canonical Rotation Matrices

Rotation Axis	Canonical Rotation Matrix
x	$\mathbf{R}^x_\gamma = \begin{bmatrix} 1 & 0 & 0 \\ 0 & \cos\gamma & -\sin\gamma \\ 0 & \sin\gamma & \cos\gamma \end{bmatrix}$
y	$\mathbf{R}^y_\gamma = \begin{bmatrix} \cos\gamma & 0 & \sin\gamma \\ 0 & 1 & 0 \\ -\sin\gamma & 0 & \cos\gamma \end{bmatrix}$
z	$\mathbf{R}^z_\gamma = \begin{bmatrix} \cos\gamma & -\sin\gamma & 0 \\ \sin\gamma & \cos\gamma & 0 \\ 0 & 0 & 1 \end{bmatrix}$

Using rotation matrices and physical and geometrical relationships, the matrix equation for the electromagnetic coupling between source and sensor is written as (6). By solving this matrix equation, it is possible to obtain the sensor induced currents based on the source currents and physical information of both source and sensor.

$$\mathbf{f_5^{(n)}} = \frac{C}{\rho^3}\mathbf{R}^\mathbf{x}_{\phi_1}\mathbf{R}^\mathbf{y}_{\theta_1}\mathbf{R}^\mathbf{z}_{\psi_1}\mathbf{R}^\mathbf{z}_{-\alpha_1}\mathbf{R}^\mathbf{y}_{-\beta_1}\mathbf{S}\mathbf{R}^\mathbf{y}_{\beta_1}\mathbf{R}^\mathbf{z}_{\alpha_1}\mathbf{f_1^{(n)}} \tag{6}$$

In (6), the $\mathbf{S}$ matrix represents the geometrical and physical coupling relationship between the sensor and the source when their x axis are aligned with zero orientation, as explained in [12]. The matrix $\mathbf{S}$ is presented in (7). The constant C, as expressed in (8), expresses the relationship between the sensor gain G, number of sensor coil turns N, and the coil surface area Ω [12].

$$\mathbf{S} = \begin{bmatrix} 1 & 0 & 0 \\ 0 & -\frac{1}{2} & 0 \\ 0 & 0 & -\frac{1}{2} \end{bmatrix} \tag{7}$$

$$C = \frac{N\Omega G}{2\pi} \tag{8}$$

Equation (6) can be also represented in terms of orientation and position rotation matrices. The orientation matrix $\mathbf{A}$ can be written as in (9), while the position matrix $\mathbf{P}$ is written as in (10).

$$\mathbf{A} = \mathbf{R}^\mathbf{x}_{\phi_1}\mathbf{R}^\mathbf{y}_{\theta_1}\mathbf{R}^\mathbf{z}_{\psi_1} \tag{9}$$

$$\mathbf{P} = \mathbf{R}^\mathbf{y}_{\beta_1}\mathbf{R}^\mathbf{z}_{\alpha_1} \tag{10}$$

Computing the matrices in (9) and (10), $\mathbf{A}$ and $\mathbf{P}$ can be written as in (11) and (12).

$$\mathbf{P} = \begin{bmatrix} \cos\alpha_1\cos\beta_1 & \sin\alpha_1\sin\beta_1 & -\sin\beta_1 \\ -\sin\alpha_1 & \cos\alpha_1 & 0 \\ \cos\alpha_1\sin\beta_1 & \sin\alpha_1\sin\beta_1 & \cos\beta_1 \end{bmatrix} \tag{12}$$

Using $\mathbf{A}$ and $\mathbf{P}$, (6) can be rewritten as (13).

$$\mathbf{f_5^{(n)}} = \frac{C}{\rho^3}\mathbf{A}\mathbf{P}^{-1}\mathbf{S}\mathbf{P}\mathbf{f_1^{(n)}} \tag{13}$$

Equation (13) describes the relationship between the source currents in a given state and the sensor induced currents. Therefore, the forward problem can be set by defining the position $P(\rho,\alpha_1,\beta_1)$ and orientation $O(\psi_1,\theta_1,\phi_1)$ of the sensor, and with known source currents for each state, the induced currents can be calculated. The inverse problem then is, given the source and sensor currents, the position P and orientation O should be defined.

3 Proposed Analytical Solution of the Electromagnetic Tracking Inverse Problem

The proposed method uses the Singular Value Decomposition to obtain position and orientation information in a electromagnetic motion tracking system similar to the one proposed in [12] and [8]. Given an n-order matrix $\mathbf{W}$, its singular value decomposition is presented in (14), where $\mathbf{U} = [\mathbf{u}_1\ \mathbf{u}_2\ \cdots\ \mathbf{u}_n]$ and $\mathbf{V} = [\mathbf{v}_1\ \mathbf{v}_2\ \cdots\ \mathbf{v}_n]$ are orthogonal matrices formed by the left ($\mathbf{u}_i$) and right ($\mathbf{v}_i$) singular vectors of $\mathbf{W}$; and $\Sigma = \mathrm{diag}(\sigma_1,\sigma_2,\cdots,\sigma_n)$ is a diagonal matrix where the singular values of $\mathbf{W}$ are decreasingly ordered [5].

$$\mathbf{W} = \mathbf{U}\boldsymbol{\Sigma}\mathbf{V}^T \tag{14}$$

The equation presented in (13) relates the information provided by the motion tracking system, generated by source ($\mathbf{f_1^{(n)}}$) and sensor ($\mathbf{f_5^{(n)}}$). Using the source excitation currents matrix $\mathbf{F_1}$ and sensor induced currents matrix $\mathbf{F_5}$ presented respectively in (4) and (5), the expression (13) can be rewritten as (15), which represents the matrix system used to determine a given position and orientation in space.

$$\mathbf{F_5} = \frac{C}{\rho^3}\mathbf{A}\mathbf{P}^{-1}\mathbf{S}\mathbf{P}\mathbf{F_1} \tag{15}$$

The matrix equation in (15) stands for a linear transformation between the source and sensor coordinate frames. The transformation matrix **T** is presented in (16).

$$\mathbf{T} = \mathbf{F_5}\mathbf{F_1}^{-1} = \frac{C}{\rho^3}\mathbf{A}\mathbf{P}^{-1}\mathbf{S}\mathbf{P} \tag{16}$$

Once **T** is known by the definition expressed in (16), the Singular Value Decomposition can be performed. To obtain the right-singular vectors in matrix **V** and the singular values matrix $\mathbf{\Sigma}$, $\mathbf{T}'\mathbf{T}$ is computed using **T** as in (16). The eigenvalues of $\mathbf{T}'\mathbf{T}$ are presented in (17), in which λ_2 is an eigenvalue with multiplicity 2.

$$\mathbf{\Lambda}_{\mathbf{T}'\mathbf{T}} = \begin{bmatrix} \lambda_1 \\ \lambda_2 \end{bmatrix} = \begin{bmatrix} \frac{C^2}{\rho^6} \\ \frac{C^2}{4\rho^6} \end{bmatrix} \tag{17}$$

Knowing the eigenvalues of $\mathbf{T}'\mathbf{T}$, the singular values σ_i can be obtained by taking their square roots. Thus, the matrix $\mathbf{\Sigma}$ can be written as in (18).

$$\mathbf{\Sigma} = \mathrm{diag}(\sigma_1, \sigma_2, \sigma_3) = \begin{bmatrix} \frac{C}{\rho^3} & 0 & 0 \\ 0 & \frac{C}{2\rho^3} & 0 \\ 0 & 0 & \frac{C}{2\rho^3} \end{bmatrix} \tag{18}$$

The corresponding unit eigenvectors for each (17) eigenvalue are presented, being (19) for λ_1, and (20) and (21) for λ_2. It can be observed that λ_2 is a complete eigenvalue, as it has a number of eigenvalues equal to its multiplicity.

$$\mathbf{v}_{\lambda_1} = \begin{bmatrix} -\cos\beta_1\cos\alpha_1 \\ -\cos\beta_1\sin\alpha_1 \\ \sin\beta_1 \end{bmatrix} \tag{19}$$

$$\mathbf{v}_{\lambda_2}^{(1)} = \begin{bmatrix} \dfrac{\sin\beta_1}{k} \\ 0 \\ \dfrac{\cos\alpha_1\cos\beta_1}{k} \end{bmatrix} \tag{20}$$

$$\mathbf{v}_{\lambda_2}^{(2)} = \begin{bmatrix} -\sin\alpha_1 \\ \cos\alpha_1 \\ 0 \end{bmatrix} \tag{21}$$

where

$$k = \sqrt{\cos^2\alpha_1\cos^2\beta_1 + \sin^2\beta_1} \tag{22}$$

Since the basis of the λ_2 eigenspace has two vectors, any linear combination of these vectors presented in (23) is also an eigenvector of $\mathbf{T}'\mathbf{T}$, consequently a right-singular vector of **T**. Therefore, any eigenvector of λ_2 eigenspace can be written as (23), where c_1 and c_2 are real scalars.

$$\mathbf{v}_{\lambda_2} = \begin{bmatrix} c_1\frac{\sin\beta_1}{k} - c_2\sin\alpha_1 \\ c_2\cos\alpha_1 \\ c_1\frac{\cos\alpha_1\cos\beta_1}{k} \end{bmatrix} \tag{23}$$

By combining the right singular vectors of **T** presented in (19) and (23) the matrix **V** can be obtained, as presented in (24), where $c_1, .., c_4$ are real scalars.

From the singular values σ_i of (18) and the right-singular matrix **V**, the position coordinates can be determined as shown in (25) for the distance ρ, (26) for the azimuth angle α_1, and (27) for the elevation angle β_1.

$$\rho = \sqrt[3]{\frac{C}{\sigma_1}} = \sqrt[3]{\frac{C}{2\sigma_2}} = \sqrt[3]{\frac{C}{2\sigma_3}} \tag{25}$$

$$\alpha_1 = \tan^{-1}\left(\frac{v_{21}}{v_{11}}\right) \tag{26}$$

$$\beta_1 = \tan^{-1}\left(\frac{v_{31}\cos\alpha_1}{-v_{11}}\right) = \tan^{-1}\left(\frac{v_{31}\sin\alpha_1}{-v_{21}}\right) \tag{27}$$

An important feature of this method is that the matrices $\mathbf{\Sigma}$ and **V** have no common variable, with **V** being in function of the position angles α_1 and β_1, while $\mathbf{\Sigma}$ is in function of the distance ρ. Therefore, the position coordinates can be determined independently using SVD over the linear transformation matrix **T**.

Since the eigenvector of λ_1 is not a linear combination as λ_2 eigenvectors, it makes the first column of **V** more predictable than the others. Because of this, the calculation of α_1 and β_1 is made with values of $\mathbf{v}_{\lambda_1}$.

One important subject in EM motion tracking systems is to determine whether a tracking value is real or spurious. Thanks to electromagnetic symmetries of the motion tracker, position angles must be studied

$$\mathbf{A} = \begin{bmatrix} \cos\psi_1\cos\theta_1 & \sin\psi_1\cos\theta_1 & -\sin\theta_1 \\ \cos\psi_1\sin\theta_1\sin\phi_1 - \sin\psi_1\cos\phi_1 & \sin\psi_1\sin\theta_1\sin\phi_1 + \cos\psi_1\cos\phi_1 & \cos\theta_1\sin\phi_1 \\ \cos\psi_1\sin\theta_1\cos\phi_1 + \sin\psi_1\sin\phi_1 & \sin\psi_1\sin\theta_1\cos\phi_1 - \cos\psi_1\sin\phi_1 & \cos\theta_1\cos\phi_1 \end{bmatrix} \tag{11}$$

within a fixed interval. This must be done because different points in the hemispherical space may show the same induction behaviour due to the magnetic field symmetry. In this case, the possible tracking angles must be limited and common sense must be used to determine the real position of the sensor [12]. Orientation angles, however, are only limited by the possible motions that the sensor can execute over his own center.

The distance ρ between source and sensor is such that only the quasi-static field component is significant, which varies with the inverse cube of the distance [12]. Therefore, ρ must be much less than the $\frac{\lambda}{2\pi}$ ratio, where λ is the wavelength of the excitation signal, and greater than the source radius r. Table 2 shows the interval of values that each variable may assume.

Table 2: Interval of Possible Position and Orientation Variables Values in an Electromagnetic Motion Tracker

Variable	Interval
ρ	$\left[r, \frac{\lambda}{2\pi}\right)$ m
α_1	$[-\frac{\pi}{2}, \frac{\pi}{2}]$ $rad.$
β_1	$[0, \frac{\pi}{2}]$ $rad.$
ψ_1	$[-\pi, \pi]$ $rad.$
θ_1	$[-\frac{\pi}{2}, \frac{\pi}{2}]$ $rad.$
ϕ_1	$[-\pi, \pi]$ $rad.$

The inverse tangent function arctan was chosen to track back the position angles in (26) and (27) because of its codomain range, that covers the α_1 and β_1 span shown in Table 2.

It must be noted that the coupling constant C must be known to determine the distance ρ between source and sensor in (25), however it can be calculated through measurements in known distances, since the singular values in $\mathbf{\Sigma}$ only hold relationships between the C and ρ.

Therefore, the position coordinates P could be obtained through SVD. In order to obtain the orientation coordinates O, the problem can be reduced to a Wahba's problem by mathematically translating the sensor signals back to the source coordinate frame [14]. As proposed by Markley [9], Wahba's problem can also be solved through SVD. A method to obtain the orientation coordinates without resorting to a coordinate transform and SVD was presented by Kuipers [8], where P and o are obtained separately.

4 Validation Methodology

The herein presented method was validated using synthetic data. A program that generates the sensor induced currents for a given set of source currents and sensor position and orientation was written. For a fixed set of source currents, 20,000 samples of uniform distribution random position and orientation signals are generated within each variable range. For test purposes the distance ρ between source and sensor was limited to 1 m, with a source radius of 3 cm. The analytical solution was applied over the linear transformation matrix $\mathbf{T}$ obtained as in (16), based solely on the source and sensor currents. Then, the true and calculated positions and orientations are submitted to a statistical error analysis.

After testing the method for a noiseless environment, a sensitivity to noise test was applied, to verify the behaviour of the system under noisy environments. Trough simulation, additive white Gaussian noise with different Signal-to-Noise Ratios (SNR) were applied over the sensor currents, getting $20,000$ samples for each SNR value. After applying the analytical solution, percentage error between true and calculated position and orientation was obtained to analyze the disturbance of the applied noise over the position calculation.

Once the error analysis had been performed, the method presented herein was compared with a previously published closed-form solution. The method chosen as the benchmark was the closed-form solution presented by Kuipers [8]. For each position and orientation, both methods were applied under different levels of noise, and their normalized root-mean-square errors are compared for each parameter. Also, the time performance of each method was compared, with both algorithms running on the same computer, using Matlab® R2017a on an Intel® Core™ i5-3470 at 3.20 GHz $\times$ 4, with an Ubuntu™ GNOME 17.04 operating system.

With this method, the validity of the analytical solution can be determined, since the induction simulation program receives random position and orientation

$$\mathbf{V} = \begin{bmatrix} -\cos\beta_1\cos\alpha_1 & c_1\frac{\sin\beta_1}{k} - c_2\sin\alpha_1 & c_3\frac{\sin\beta_1}{k} - c_4\sin\alpha_1 \\ -\cos\beta_1\sin\alpha_1 & c_2\cos\alpha_1 & c_4\cos\alpha_1 \\ \sin\beta_1 & c_1\frac{\cos\alpha_1\cos\beta_1}{k} & c_3\frac{\cos\alpha_1\cos\beta_1}{k} \end{bmatrix} \tag{24}$$

Table 3: Error Analysis Between True and Calculated Position and Orientation Values in a Noiseless Environment

Variable	RMS Error	Normalized RMS Error (%)
ρ	$3.8970 \cdot 10^{-17}\ m$	$1.1102 \cdot 10^{-14}$
α_1	$7.3618 \cdot 10^{-12\circ}$	$1.4178 \cdot 10^{-11}$
β_1	$6.8372 \cdot 10^{-14\circ}$	$2.6645 \cdot 10^{-13}$
ψ_1	$1.3136 \cdot 10^{-11\circ}$	$1.2623 \cdot 10^{-11}$
θ_1	$1.3044 \cdot 10^{-12\circ}$	$2.5091 \cdot 10^{-12}$
ϕ_1	$1.3179 \cdot 10^{-11\circ}$	$1.2679 \cdot 10^{-11}$

Table 4: Error Analysis Between True and Calculated Position and Orientation Values in a Noisy Environment

SNR (dB)	Error	Variable					
		ρ	α_1	β_1	ψ_1	θ_1	ϕ_1
20	RMS	7.6317 mm	35.1831°	33.0100°	59.7902°	5.4953°	61.0573°
	NRMS (%)	2.6349	67.3264	127.0473	57.4196	10.5655	58.9741
	R^2	0.9993	0.5979	0.2311	0.6981	0.9889	0.6823
40	RMS	0.76280 mm	13.1699°	12.7124°	23.3040°	0.5448°	26.1498°
	NRMS (%)	0.2652	25.3544	48.9295	22.4509	1.0516	25.0498
	R^2	1.0000	0.9368	0.7920	0.9502	0.9999	0.9383
60	RMS	75.968 μm	5.5624°	5.3552°	8.7455°	0.0545°	7.6531°
	NRMS (%)	0.0263	10.7489	20.6300	8.4101	0.1054	7.3597
	R^2	1.0000	0.9885	0.9585	0.9929	1.0000	0.9946
80	RMS	7.5370 μm	2.2475°	2.1777°	1.7551°	0.0054°	5.7274°
	NRMS (%)	0.0026	4.3118	8.3854	1.6889	0.0105	5.5155
	R^2	1.0000	0.9981	0.9930	0.9997	1.0000	0.9970
100	RMS	0.75558 μm	0.0496°	0.0003°	0.0463°	0.0005°	0.0462°
	NRMS (%)	0.0003	0.0955	0.0013	0.0447	0.0010	0.0448
	R^2	1.0000	1.0000	1.0000	1.0000	1.0000	1.0000

values, delivering only a set of source and sensor currents, without any other information in advance, such as last sensor position, required in other methods. The analytical solution must track them directly from these current values in noisy and noiseless environments, being also robust to parameter uncertainty, making it a fair validation test for the presented method, due to its randomness.

5 Validation Results

5.1 Error Analysis

Table 3 shows the description of the error between true and calculated values for a random motion simulation for each of the six degrees-of-freedom after 20,000 samples for a noisy environment, while Table 4 shows the error description for noisy environments.

From the presented results, it can be seen that the analytical solution successfully calculated the true position and orientation with mean error equal to $1.5387 \times 10^{-17}\%$ and mean standard deviation of $8.7965 \times 10^{-16}\%$, based only on the source and induced sensor currents in a noiseless environment. Such small values of error can be taken as zero without any loss of generality. Therefore, the analytical solution is valid for the whole interval of possible tracking variables, having a very small error between the calculated value and the true position and orientation.

Observing the results presented in Table 4, it can be seen that the analytical solution is fairly robust to additive white Gaussian noise for signal-to-noise ratios greater than 60 dB. The estimation of the distance ρ suffer less interference on the error, since it can be obtained through an average of the different forms to obtain it as shown in (25). With $SNR = 80$ dB, all the variables have sufficiently small errors, while in $SNR = 100$ dB it is almost negligible. It must be observed that the elevation angle β_1 presents the largest error value of all measurements, due to its dependency of the azimuth angle α_1, which in noisy environments, greatly increases the elevation error.

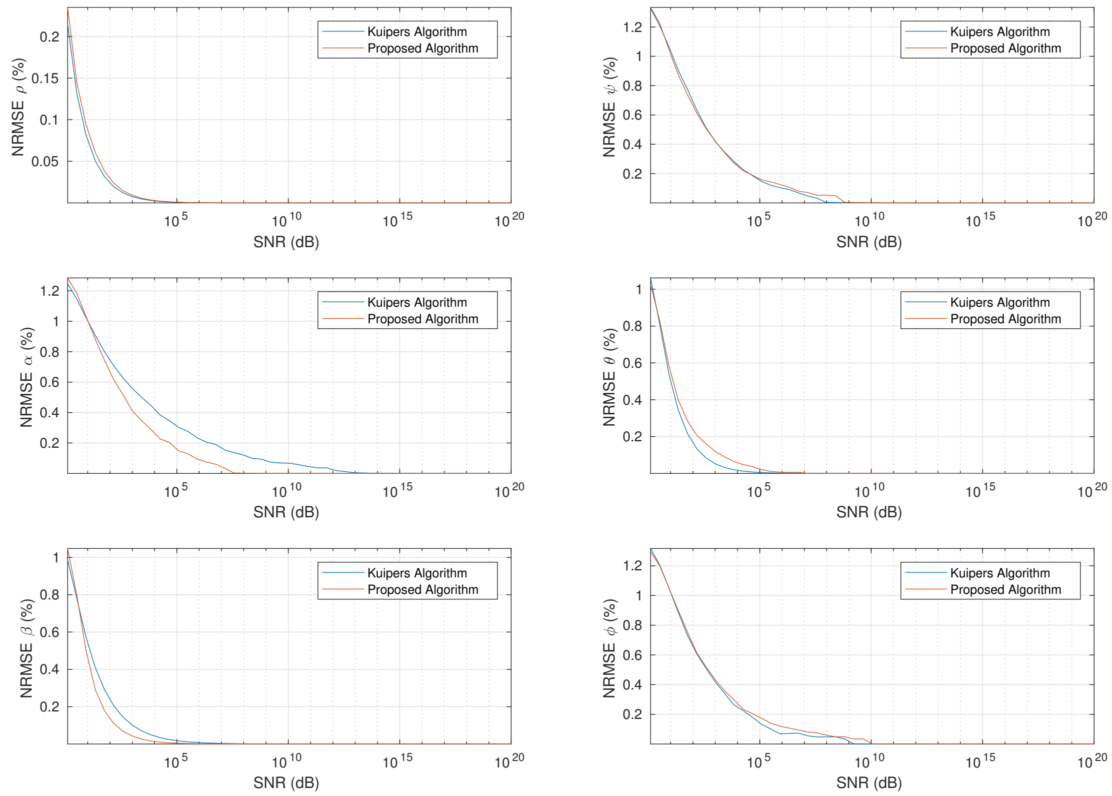

Figure 2: Normalized root-mean-square error of each measurement when applying the proposed an Kuipers' method [8] under different noise levels.

Aside from the environmental noise over the sensor, parameter uncertainty is another source of error that may occur during the calculation. Thus, the robustness of the method to parameter uncertainty must also be assessed.

5.2 Benchmarking

Figure 2 presents the normalized root-mean-square errors (NRMSE) for each measurement when applying the proposed method and the closed-form solution presented by Kuipers [8], under different noise levels, while Figure 3 shows the histogram of the elapsed time for each algorithm to obtain all measurements.

From Figure 2, it can be observed that, even though the two methods have different mathematical approaches, both have comparable results under different noise levels. Even though the difference is slim, the proposed algorithm retrieves a better estimate of the position angles α and β, while Kuipers' algorithm retrieves a more accurate estimate of the orientation angle θ. All other measurements are have very close NRMSEs.

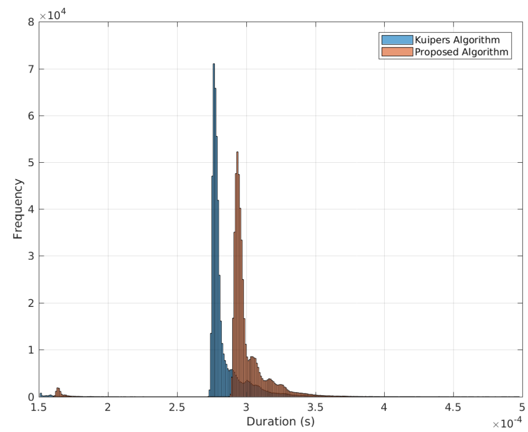

Figure 3: Histogram of the elapsed time for each inversion when applying the proposed an Kuipers' method [8] under different noise levels.

Analyzing the time performance, both algorithms have have similar performances, with Kuipers' method having an advantage of 17 μs if the sample modes are compared.

With this benchmark analysis it can be seen that the proposed method has a performance comparable to the closed-form solution presented by Kuipers [8].

6 Conclusions

This article proposes an alternative analytical solution for the electromagnetic motion tracking system problem using Singular Value Decomposition. The method was validated through simulation using uniformly distributed random position and orientation values and benchmarked against the closed-form solution proposed by Kuipers. The proposed analytical method retrieved very good results, calculating position and attitude with very low errors and error variances, attesting its efficacy. The analytical method also presented good robustness to additive Gaussian noise. However, for more accurate solutions, it is recommended to remove possible sources of noise of the surrounding environment and apply noise filtering techniques over the received signal.

When compared with Kuipers' method, the presented algorithm yielded results that are comparable with the benchmark, having a slightly better result for some position angles under high levels of noise. The time performance of the presented method is also comparable to the one presented by Kuipers' algorithm, with a narrow advantage of 17 μs for the latter.

This method is presented as an alternative solution to the electromagnetic motion tracking problem and opens a venue for future improvement on the algorithm and different applications.

References:

[1] C. A. Balanis, *Antenna Theory: Analysis and Design*, 3rd ed. Wiley-Interscience, 2005.

[2] J. V. Condell, G. Moore, and J. Moore, "Software and Methods for Motion Capture and Tracking in Animation," in *CGVR*. Citeseer, 2006, pp. 3–9.

[3] A. M. Franz, T. Haidegger, W. Birkfellner, K. Cleary, T. M. Peters, and L. Maier-Hein, "Electromagnetic Tracking in MedicineA Review of Technology, Validation, and Applications," *Medical Imaging, IEEE Transactions on*, vol. 33, no. 8, pp. 1702–1725, 2014.

[4] X. Ge, Y. Wang, N. Ding, X. Wu, Y. Wang, and Z. Fang, "An Electromagnetic Tracking Method Using Rotating Orthogonal Coils," *IEEE Transactions on Magnetics*, vol. 48, no. 12, pp. 4802–4810, Dec 2012.

[5] G. H. Golub and C. Reinsch, "Singular value decomposition and least squares solutions," *Numerische mathematik*, vol. 14, no. 5, pp. 403–420, 1970.

[6] J. Huang, T. Mori, K. Takashima, S. Hashi, and Y. Kitamura, "IM6D: magnetic tracking system with 6-DOF passive markers for dexterous 3D interaction and motion," *ACM Transactions on Graphics (TOG)*, vol. 34, no. 6, p. 217, 2015.

[7] V. V. Kindratenko, "A survey of electromagnetic position tracker calibration techniques," *Virtual Reality*, vol. 5, no. 3, pp. 169–182, 2000.

[8] J. Kuipers, "Method and apparatus for determining remote object orientation and position," Patent, May 3, 1988, uS Patent 4,742,356.

[9] F. L. Markley, "Attitude determination using vector observations and the singular value decomposition," *The Journal of the Astronautical Sciences*, vol. 36, no. 3, pp. 245–258, 1988.

[10] K. O'Donoghue, D. Eustace, J. Griffiths, M. O'Shea, T. Power, H. Mansfield, and P. Cantillon-Murphy, "Catheter position tracking system using planar magnetics and closed loop current control," *Magnetics, IEEE Transactions on*, vol. 50, no. 7, pp. 1–9, 2014.

[11] E. Poulin, E. Racine, D. Binnekamp, and L. Beaulieu, "Fast, automatic, and accurate catheter reconstruction in hdr brachytherapy using an electromagnetic 3d tracking system," *Medical Physics*, vol. 42, no. 3, pp. 1227–1232, 2015. [Online]. Available: http://dx.doi.org/10.1118/1.4908011

[12] F. H. Raab, E. B. Blood, T. O. Steiner, and H. R. Jones, "Magnetic Position and Orientation Tracking System," *IEEE Transactions on Aerospace and Electronic Systems*, vol. AES-15, no. 5, pp. 709–718, Sept 1979.

[13] H. Ren and P. Kazanzides, "Investigation of Attitude Tracking Using an Integrated Inertial and Magnetic Navigation System for Hand-Held Surgical Instruments," *IEEE/ASME Transactions on Mechatronics*, vol. 17, no. 2, pp. 210–217, April 2012.

[14] G. Wahba, "A Least Squares Estimate of Satellite Attitude," *SIAM Review*, vol. 7, no. 3, pp. 409–409, 1965.

[15] J. Zhou, E. Sebastian, V. Mangona, and D. Yan, "Real-time catheter tracking for high-dose-rate prostate brachytherapy using an electromagnetic 3D-guidance device: A preliminary performance study," *Medical Physics*, vol. 40, no. 2, pp. 021 716–n/a, 2013, 021716. [Online]. Available: http://dx.doi.org/10.1118/1.4788641